Analysis and microelectronic design of tubular electrode arrays intended for chronic, multiple single-unit recording from captured nerve fibres

G. E. Loeb   **W. B. Marks**   **P. G. Beatty**

Laboratory of Neural Control, National Institutes of Health/NINCDS   University of Chicago, School of Medicine, Chicago, Ill., USA
Bethesda, Mnd. 20014, USA

Abstract—*The paper discusses proposals for recording multiple single-unit potentials from nerve fibres that become captured in an array of tube electrodes. Capturing may be through regeneration of cut fibres or by placement of dissected filaments into grooves which are then covered. The factors contributing to signal-to-noise ratios obtainable with this type of electrode are discussed. The design, construction and bench-test results are given for an electrode array in which thin-film microelectronic techniques are used to build a densely packed, flexible, 3-dimensional electrode array consisting of a bundle of plastic tubes with flat metal contacts at midtube.*

Keywords—*Chronic recording, Microelectrode arrays, Neurophysiology*

Introduction

THE DIFFICULTIES of adapting the classical metal microelectrode to chronic recording are legion, particularly when multiple, closely spaced probes are desired. The electrodes are fragile, their electrical and physical properties inconsistent, and their manipulation and positioning quite tedious. 'Floating' microelectrodes (SALCMAN and BAK, 1973) improve chronic-recording stability, but it is still not possible to guarantee holding a single unit for more than a day or so.

Ideally, to maximise the number of information channels and minimise the intrusion on the nervous system, it would be desirable to have several neurons simultaneously present on each of several channels. With high signal-to-noise ratios and stable or only slowly changing waveforms, one could make use of any of several waveform analysers and separators previously described (KENT, 1971; SCHMIDT, 1971; GLASER and MARKS, 1968). An attempt to achieve such a data stream was made by GERSTEIN and CLARK (1964) who designed a single electrode with multiple exposed metal patches, but their design suffers the usual problems of discrete microelectrodes, plus an additional signal-to-noise attenuation caused by averaging signals over several patches.

In this paper, we explore previously proposed techniques for achieving a solution to these problems by capturing nerve fibres in tubes, either by allowing them to regenerate through tubes (MARKS, 1969) or by inserting them into grooves which are subsequently sealed (HOFFER et al., 1973; BRINDLEY, 1972). This configuration has certain inherent properties which should both stabilise spatial relationships between electrodes and nerve fibres

and increase the signal-to-noise ratios obtainable extracellularly.

Peripheral nerves (GUTH, 1956) as well as the optic nerve of lower vertebrates (ATTARDI and SPERRY, 1963) will regenerate if cut and re-establish functional connections. MARKS found that peripheral nerve bundles of bullfrogs (1969) and rats (personal communication) will regenerate through sponges and tubes of various metals and plastics, although rat sciatic nerve fibres appear to be somewhat limited in their ability to fill densely a narrow tube, because of the more rapid proliferation of Schwann cells. Mammalian and amphibian c.n.s. fibres appear either not to regenerate, or to regenerate around rather than across cuts (MARKS, 1972 *a*, *b*, *c*, and *d*). However, c.n.s. fibres have been seen to slide spontaneously into deep, narrow grooves ($25 \times 5 \, \mu m$) in inert plastic implants (unpublished).

Recently, MANNARD et al. (1974) constructed a tubular regeneration electrode by mechanical drilling through silver wires embedded in Epon. Their array of 10 such tubes, $100 \mu m$ in diameter and $700 \, \mu m$ long, successfully recorded 50 to $150 \, \mu V$ multiunit potentials from regenerated Xenopus sciatic motor fibres.

This paper analyses the neuronal and electrode parameters that are theoretically important in recording from nerve fibres in tubes and describes a fabrication technique for regeneration tube arrays which appears to be adaptable to a variety of electrode approaches. The difficulties in hand manufacture of electrode arrays, as well as the inherent limitations of geometry and packing of discrete wires, has led us to develop techniques of thin-film microelectronics in constructing arrays of tubular electrodes. Such techniques are beginning to find uses in neurophysiology for both *in vivo*

(Wise et al., 1970) and in vitro (Thomas et al., 1972) multiple microelectrode arrays. Llinas et al. (1973) have proposed a design incorporating first-stage amplification and multiplexing on a silicon wafer with holes for regenerating fibre capture, although this has yet to be built.

With planar construction, bringing leads out in the same plane as the tubes allows stacking of rows of tubes so that the surface seen by the cut nerve fibres has a greater density of channels. Also, the basic technique of photolithographic fabrication allows fine control over such parameters as tube size and shape and number and position of contacts per tube to take advantage of whatever biologic factors may govern nerve regeneration.

Theoretical considerations

Metabolic limitations on tube length

Since nerve fibres function as virtual constant current sources, the extracellular potential recordable at the centre of a long narrow tube surrounding the fibre will increase with an increasing length of the tube and decreasing diameter. However, the returns from increasing length begin to diminish as the tube reaches the wavelength of the action potential (3 to 30 mm for both myelinated and unmyelinated fibres (Paintal, 1966; 1967). If blood vessels do not grow through the tubes, oxygen diffusion may become the limiting factor for tube length. The consumption of oxygen can be considered independent of oxygen concentration down to low levels (4 mm Hg) (Elliott and Henry, 1946), so that the tube length must not exceed the value L for which the oxygen concentration at the midpoint vanishes. For cylindrical geometry with uniform oxygen consumption of densely packed tissue, this limiting length (Hober, 1945) is

$$L = (8DP/E)^{\frac{1}{2}} \quad . \quad . \quad . \quad . \quad . \quad . \quad (1)$$

Using $P = 0 \cdot 1$ atm. (partial pressure of capillary bed as mean of arterial and venous O_2 tension), $D = 1 \cdot 15 \times 10^{-5}$ ml O_2/cm min atmos (diffusion constant for connective tissue) (Krogh, 1919 and $E = 3 \cdot 73 \ 10^{-4}$ ml O_2/g min (metabolic rate for frog sciatic nerve at 20°C stimulated to fire at 100 Hz) (Brink et al., 1952) gives $L = 1 \cdot 57$ mm. Using $E = 2 \cdot 17 \times 10^{-3}$ ml O_2/g min for rat saphenous nerve at 37°C (Larrabee and Bronk, 1952) and correcting D by $1\%/°C$ (Krogh, 1919), gives $L = 0 \cdot 7$ mm. The density of regenerated tissue may be less in the tubes than within normal nerves, but the metabolic rate of regenerating tissue is probably greater. Thus the foregoing figures merely set approximate upper bounds for the length of cylindrical tubes in which nerve fibres can survive without accompanying blood vessels.

Signal-to-noise optimisation of tubular electrodes

We shall assume that the overall tube-electrode length and tube diameter are fixed by metabolic, mechanical, signal processing and experimental considerations. Within those constraints, we may optimise the expected signal-to-noise ratio of our electrode by varying the percentage of the tube inside wall surface occupied by the metallic electrode pickup, achieved by varying L_x in the planar design diagrammed in Fig. 1.
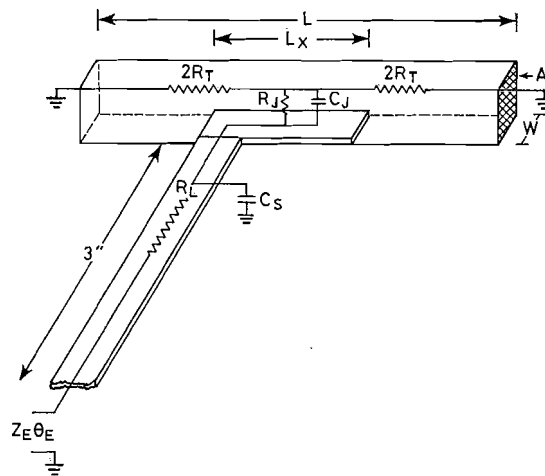

Fig. 1 Tubular-electrode configuration with equivalent-circuit elements and dimensions defined (see table 1)

The signal is proportional to the effective resistance of the fluid in the tubes on either side of the conducting metal patch.

$$R_T = \frac{\rho}{4A'} (L - L_x) \quad . \quad . \quad . \quad . \quad . \quad . \quad (2)$$

The thermal (Johnson) noise is proportional to the square root of the real component of the total electrode impedance (fluid column plus metal/electrolyte junction).

$$Z_R = \frac{\hat{R}}{WL_x[1 + (2\pi F \hat{R}\hat{C})^2]} + R_T \quad . \quad . \quad (3)$$

The specific resistivity of the tissue in the tubes (ρ) is likely to fall somewhere between that of extracellular fluid (0·8 MΩμm for frog, 0·65 MΩμm for mammals) and that of densely packed, longitudinally oriented white matter, which is about three times higher [2·45 MΩμm for frog sciatic nerve (Tasaki, 1964)]. Over that range of values for ρ in a tube with dimensions L, A, and W, as listed in Table 1, and using either our own or Robinson's (1968) values of $\hat{R} = 800$ MΩμm² and $\hat{C} = 0·2$ pF/μm², the ratio $R_T/\sqrt{Z_R}$ is never less than 90% of its maximum for any L_x between 50 and 180 μm. In the electrode design described here, L_x was set at 150 μm. In the calculations in Table 1,

Table 1. Tubular-electrode dimensions and electrical parameters

	Amphibian	Mammalian	
$L = 950 \,\mu m$			(tube length)
$L_X = 150 \,\mu m$			(electrode-patch length)
$W = 15 \,\mu m$			(electrode-patch width)
$A = 225 \,\mu m^2$			(tube cross-sectional area)
$C = 0 \cdot 2 \,pF/\mu m^2$			(capacity per unit area of metal/electrolyte junction)*
$C_J = 450 \,pF$			(capacitance of electrode patch to electrolyte)
$R = 7000 \,M\Omega\mu m^2$			(resistivity of metal/electrolyte junction)*
$R_J = 3 \cdot 1 \,M\Omega$			(resistance of electrode patch to electrolyte)
$C_S < 50 \,pF$			(shunt capacitance along leads)*
$R_L < 1 \,k\Omega$			(lead resistance)*
$F = 1 \,kHz$			(frequency of test sinewave)
$B = 20 \,kHz$			(bandwidth of recording amplifier)
ρ	$0 \cdot 80 \,M\Omega\mu m$	$0 \cdot 65 \,M\Omega\mu m$	(resistivity of Ringer's solution)
Z_E	$0 \cdot 83 \,M\Omega$	$0 \cdot 71 \,M\Omega$	(overall tube-electrode impedance)
R_T	$0 \cdot 71 \,M\Omega$	$0 \cdot 58 \,M\Omega$	(resistance of Ringer's solution filled tube)
Z_R	$0 \cdot 75 \,M\Omega$	$0 \cdot 62 \,M\Omega$	(real component of Z_E)
E_N	$15 \cdot 6 \,\mu V$	$14 \cdot 0 \,\mu V$	(r.m.s. Johnson noise associated with Z_R)

* derived from our empirical measurements on samples of the materials employed.

ρ is that of the test solutions, comparable to extracellular fluid resistivity.

The root-mean-square Johnson noise E_N is given by

$$E_N = (4kTBZ_R)^{\frac{1}{2}} \quad \ldots \quad \ldots \quad \ldots \quad (4)$$

where k is the Boltzman constant, T is the Kelvin temperature, and B is the recording amplifier bandwidth (20 kHz assumed, see below). The Johnson noise of a tube filled with fibres would be up to 1·7 times higher.

Signal amplitudes for various fibres in tubes

A comprehensive derivation of the signals to be obtained from unmyelinated amphibian nerve fibres under a variety of electrode configurations has been presented by STEIN and PEARSON (1971). From their curves of triphasic waveforms (single electrode in symmetrical insulating tube), we have calculated by their method that a $3 \cdot 5 \,\mu m$ fibre conducting at 1 m/s would generate a $4 \cdot 42$ mV peak signal at the centre of our tubular electrodes ($L = 950 \,\mu m$, $A = 225 \,\mu m^2$). Thus the tubular electrode might be useful for capturing the re-relatively large currents generated by nonsaltatory conduction in unmyelinated fibres, producing large signals in these normally difficult to record from small fibres. Signals would, however, be expected to drop off rapidly with decreasing fibre diameter, with a factor of d^2 for the transconductance ratio of fibre to tube when the tube is longer than the wavelength.

For unmyelinated mammalian fibres, we are at a complete loss for predictive data. The above data is based on squid giant axon waveform parameters at 20°C and their applicability even to the small fibres of higher cold-blooded animals may be questioned.

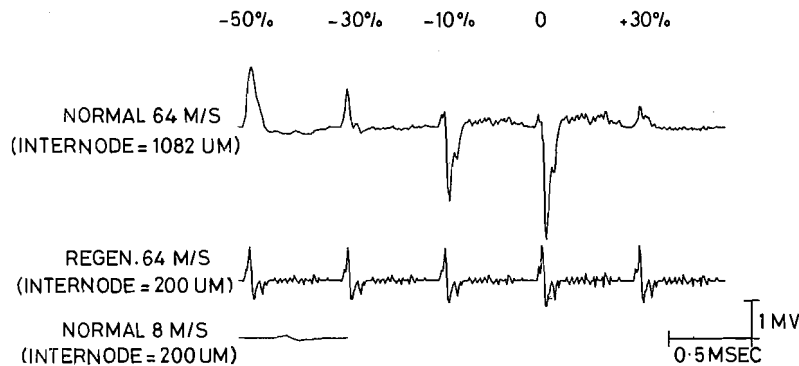PREDICTED SIGNALS FROM FIBRES AT VARIOUS NODE OFFSETS:

Fig. 2 Theoretical signals which would be recorded from different mammalian fibres in a tube electrode with the dimensions indicated in Table 1, densely packed with nerve fibres.

Action potentials are shown propagating from left to right, with the node of Ranvier offset by various percentages (top) of the internode length from the centre electrode

A detailed discussion of our method for calculating tube-electrode waveforms for both mammalian and amphibian myelinated fibres is published elsewhere (MARKS and LOEB, 1976). It is similar to the method for unmyelinated fibres in which the second difference between the intra-axonal potentials at the centre and ends of the tube is scaled by the ratio of axon-to-tube longitudinal conductivity. In adapting this method to a regeneration electrode, we have assumed that the only significant fibre change is internodal length. In normal fibres, both conduction velocity and internode length are nearly proportional to fibre diameter over a wide range of sizes. In regenerated fibres, conduction velocities approach normal with a time constant of about 100 days (SANDERS and WHITTERIDGE, 1946), but internode length ceases to depend on fibre diameter and assumes its embryonic value, equal to that of the smallest normal fibres (VIZOSO and YOUNG, 1948; HISCOE, 1947).

Fig. 2 shows the theoretical signal waveforms which would be recorded in a tube with the dimensions given in Table 1, filled with fibres having an aggregate longitudinal resistivity $\rho = 2 \cdot 4 \, M\Omega\mu m$. The top trace shows the signals for a normal (intact) 64 m/s mammalian fibre (outside diameter $= 11 \cdot 5 \, \mu m$, internode length $= 1092 \, \mu m$) with the node of Ranvier positioned at five different distances from the centre of the tube (0% indicates node at centre electrode, -50% indicates node displaced 50% of the internode length to the left of the centre point with the direction of propagation from left to right). When the internode length is greater than the tube length, it is possible to have the node closest to the electrode positioned anywhere from the centre to completely outside the tube, producing the large range of both waveforms and amplitudes seen. The same-diameter regenerated fibre, with a 200 μm internode length (middle trace), has comparable signal amplitudes but they are much more consistent because there must always be one node within 100 μm of the centre.

The bottom trace shows the signal that would be expected from an 8 m/s fibre, which would be expected to have a 200 μm internode whether normal or regenerated, and thus has little signal variance with node position (not shown). The signal amplitude for this 2·1 μm-diameter fibre is about 100 μV peak-to-peak, which would be marginally detectable above noise (14 μV r.m.s. $\times 1 \cdot 7$ to correct for longitudinal resistivity, $\times 3$ to convert to peak-to-peak noise $= 71 \, \mu V$). Note the very rapid time course of these signals, which has caused us to select 20 kHz for the recording bandwidth which might be required to avoid attentuating the signals or degrading shape information useful for sorting.

It seems probable that the tubular electrode analysed here is about the smallest in diameter that one would wish to construct and that there may be applications in which considerably larger tubes are used, particularly where it is intended that intact fibres be surgically placed into grooves which are subsequently sealed into tubes. Such larger tubes would be considerably easier to manufacture by microelectronic or other techniques. The length limitation imposed by the diffusion of metabolites in a tube without intrinsic blood supply is unaffected by enlarging the cross-sectional area (eqn. 1), so we may anticipate that large tubes will have decreased ratios of length to cross-sectional area, with reductions of signal size predicted by eqns. 2 and 4. Even larger diameter tubes in which intact nerve filaments containing blood vessels might be placed can only have a moderate (eight-fold) increase in useful tube length until the wavelength of the action current is reached. In fact, recent experience indicates that such tubes still produce adequate signal-to-noise values (HOFFER et al., 1973), but precise predictions become difficult because of the anisotropy of nerve fibre bundles (TASAKI, 1964; PLONSEY, 1974) resulting in the dominance of local current gradients (MARKS and LOEB, 1976).

Electrode-array design and construction

In microelectronics, layers of conductors and insulators are sequentially applied and selectively removed photolithographically, much like the production of very small printed circuits. Although, traditionally, such devices have no significant three-dimensionality, we have combined thick electroplating, potting and stacking to construct a
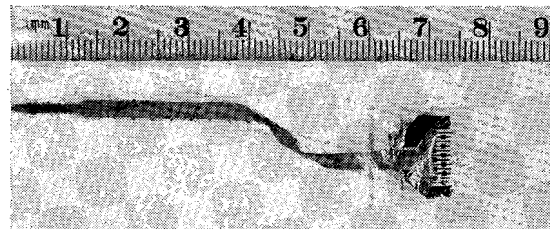

Fig. 3 Single-layer cable for implanting, showing electrode array end at left, flexible ribbon cable, and contact area mounted on glass at right

3-dimensional array of tube electrodes. The resulting device is a 50 μm-thick plastic strip with 12 gold-titanium thin-film contacting pads at one end, connected by 12 parallel leads to the individual tube electrodes 80 mm away at the other end of the strip (see Fig. 3). The electrodes (platinum plated over the Au-Ti metallisation) form part of the floor of 12 plastic tubes running through the plastic strip in the same plane, but at right angles to the leads. The leads are insulated with a permanent layer of stabilised photoresist as they cross under all the tubes, except the ones where they terminate as electrode patches. The tubes themselves are 10 to 15 μm high, 10 to 15 μm wide, and may be 300 to

1200 μm long. They are spaced on 25 μm centres (see Fig. 4). The highly flexible strip circuits may be stacked giving large numbers of electrodes. Each layer from the top is slightly longer, so that when the rows of tubes are lined up over each other, all the contact pads at the other end are accessible. After initial tooling and mask preparation, five 12-tube arrays can be made in about 10 man-hours by an experienced microelectronics technician.
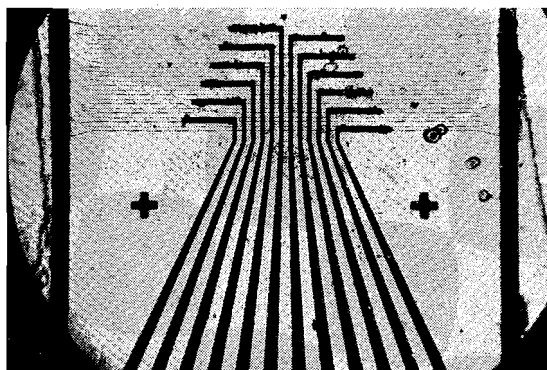

Fig. 4 Photomicrograph of a single-layer electrode array after 30 days in saline (room temperature). Features from left are: rough-cut edge of array; common electrode which borders ribbon cable along its entire length, and seen here running vertically across the floor of the 'front porch', which begins at the cut edge; staggered tapered walls which divide front porch into 12 tube-like channels; metal-electrode patches on floor of six tubes; triangular cross-over region, where leads from electrodes pass under the insulation patch (invisible here) as tubes pass over; electrode patches in other six tubes; tubes leading to right front porch with second common electrode, rough cut edge of the array. The tubes are approximately 1000 μm long and are spaced 25 μm apart centre-to-centre

Each single layer starts as a substrate of 15 μm thick Parylene-C (Union Carbide Corp., New York) vapour deposited on temporary glass carrier slides (LOEB et al., in press, a and b). The initial Au-Ti metallisation is photolithographically formed, electroplated with platinum distally, and covered with the photolithographed insulating photoresist as shown in Fig. 5. A transparent overcoat of evaporated nickel provides conductivity for electroplating the nickel bar pattern through a photoresist mask; it is then etched away leaving the isolated bars seen in Fig. 5.

A number of such completed layers are peeled from their glass carriers and aligned and sandwiched together with epoxy resin which flows around the nickel bars. Trimming the edges exposes these bars which are etched out with nitric acid, leaving the multitube device illustrated in Fig. 6.

Test results

The schematic diagram in Fig. 1 represents the approximate equivalent circuit of a tubular electrode. Measurements in our laboratory of the conductivity of test saline and of the junction properties at 1 kHz (sinewave) of the platinum electroplate employed predict the values indicated for the various components of the complex impedance. It should be noted that these results differ significantly from the commonly referenced figures of ROBINSON (1968) for platinum black, as discussed previously.

Tests on electrode assemblies of approximately the dimensions indicated (Table 1) yielded impedances of approximately 0·8 MΩ at a voltage phase lag of approximately 30°, consistent with the predicted results of 0·83 MΩ at 22°. The impedance measured between two adjacent electrodes in
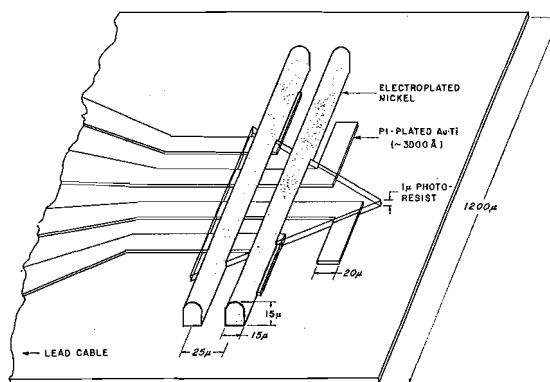

Fig. 5 Four typical electrodes during fabrication. The triangular patch of insulating photoresist has been applied over the cross-over region of the platinum-plated gold/titanium lead lines. Only two of the nickel bars which will eventually be etched out to form tubes are shown. Each lies centred on its electrode patch of Pt-plated Au-Ti and extends from one side of the 1200 μm-wide plastic substrate to the other, passing over the insulation patch. At their ends (not shown), the nickel bars become wider and join so that, when etched out, a large open area is formed

saline is approximately 1·5 MΩ (at 1 kHz), indicating approximately 24 MΩ isolation between electrodes, or 3% crosstalk for the worst shunt position at the electrode patches. Tests were conducted by monitoring the voltage between the electrode lead and a large common platinum electrode, in the bath or between two electrode leads, while passing approximately 0·01 μA constant-current sinewaves via a large series resistor and d.c. blocking capacitor.

Initial implantations were unsuccessful because of technical problems involving anchoring to the nerve and connectors. At present, this technique

for recording is being pursued actively by one of us (WBM) with concentration on placing uncut fibres into split tubes. Until an optimum configuration is found, discrete wire techniques are being used to facilitate design changes.

References

ATTARDI, D. G. and SPERRY, R. W. (1963) Preferential selection of central pathways by regenerating optic nerve fibres. *Exp. Neurol.* **7,** 46–64

BRINDLEY, G. S. (1972) Electrode arrays for making long-lasting electrical connexion to spinal roots. *J. Physiol. (Lond)* **222,** 135–136

BRINK, F., BRONK, D. W., CARLSON, F. D. and CONNELLY, C. M. (1952) The oxygen uptake of active axons. Cold Spring Harbor Symposium on Quantitative Biology. **17,** 53–67

ELLIOTT, K. A. C. and HENRY, M. (1946) Studies on the metabolism of brain suspensions, III. Respiration at low oxygen tension. *J. Biol. Chem.* **163,** 351–359.

GERSTEIN, G. L. and CLARK, W. A., (1964) Simultaneous studies of firing patterns in several neurons. *Science* **143,** 1325–1327

GLASER, E. M. and MARKS, W. B. (1968) On-line separation of interleaved neuronal pulse sequences. *Data acquisition and processing in biology and medicine* **5,** Pergamon Press, New York

GUTH, L. (1956) Regeneration in the mammalian peripheral nervous system. *Physiol. Rev.* **36,** 441–478

HISCOE, B., (1947) The distribution of nodes and incisures in normal and regenerated nerve fibres. *Anat. Rec.* **99,** 447–475

HOBER, R. (1945) *Physical chemistry of cells and tissues* Blakiston, Philadelphia, 375–383

HOFFER, A., MARKS, W. B. and RYMER, W. Z. (1973) Groove electrode arrays for chronic multichannel recording from dorsal root fibres. *Abst. of Soc. for Neuroscience*, 3rd Annual Meeting

KENT, E. W. (1971) An educable wave form recognition program suitable for on-line discrimination of extracellular single units. *EEG Clin. Neurophysiol.* **31,** 618–620

KROGH, A. (1919) The rate of diffusion of gases through animal tissues, with some remarks on the coefficient of invasion. *J. Physiol. (Lond)* **52,** 391–408

LARRABEE, M. G. and BRONK, D. W. (1952) Metabolic requirements of sympathetic neurons. Cold Spring Harbor Symposium on Quantititive Biology **17,** 245–266

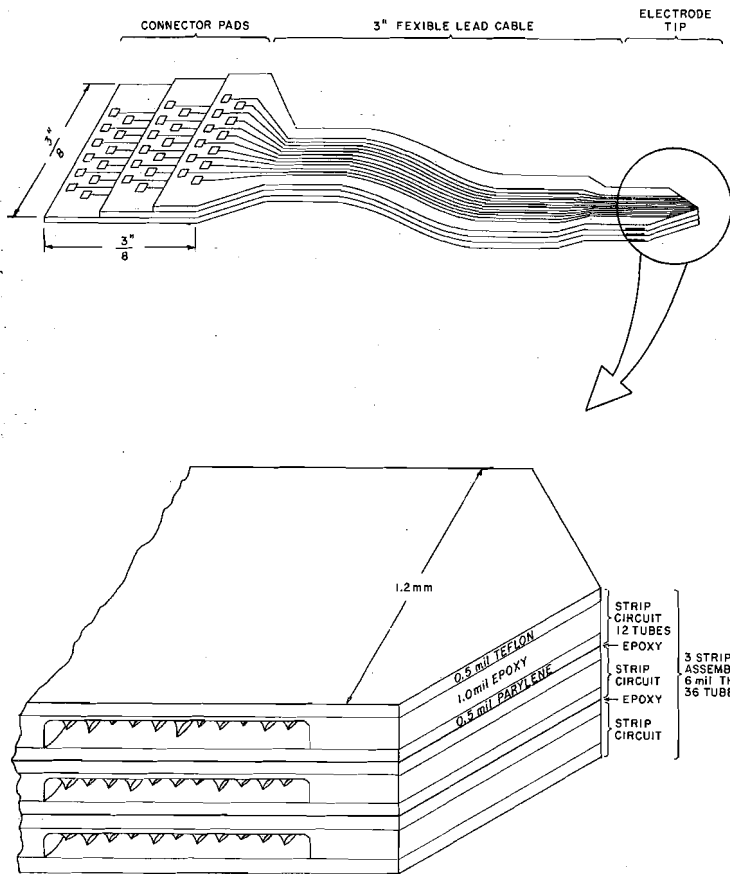LLINAS, R., NICHOLSON, C. and JOHNSON, K. (1973)

Fig. 6 Schematic of three arrays stacked so that connector pads from all 36 electrodes are accessible. The electrode tip detail shows the large open 'front porch' of each layer dividing into twelve tube-like channels farther in

Implantable monolithic wafer recording electrodes for neurophysiology. In *Brain unit activity during behaviour*, M. I. PHILLIPS, (Ed). Charles C. Thomas, Springfield.

LOEB, G. E., BAK, M. J. and SALCMAN, M. (*a*) Parylene as a chronically stable, biocompatible microelectrode insulator. *IEEE Trans.* **BME** (in press)

LOEB, G. E., WALKER, A. E., UEMATSU, S. and KONIGS-MARK, B. W. (*b*) Histologic reaction to various conductive and dielectric films chronically implanted in the subdural space. *J. Biomed. Mat. Res.* (in press)

MANNARD, A., STEIN, R. B. and CHARLES, D. (1974) Regeneration electrode units: Implants for recording from single peripheral nerve fibres in freely moving animals. *Science* **183**, 547–549

MARKS, A. F. (1969) Bullfrog nerve regeneration into porous implants. *Anat. Rec.* **163**, 226

MARKS, A. F. (1972*a*) Optic tract regeneration in the adult rat. *Abst. of Soc. for Neuroscience*, 2nd Ann. Meeting, Houston, Texas

MARKS, A. F. (1972*b*) Regenerative reconstruction of a tract in a rat's brain. *Exp. Neurol.* **34**, 455–464

MARKS, A. F. (1972*c*) Regenerative reconstruction of tracts in the adult rat's brain. *Anat. Rec.* **172**, 363

MARKS, A. F. (1972*d*) Regeneration reconstruction of tracts in the adult rat's brain. *Abst. of 1972 Anatomy Meeting*, Dallas, Texas

MARKS, W. B. (1965) Some methods of simultaneous multiunit recording. Proceedings of the symposium on information processing in sight sensory systems, California Institute of Technology, Pasadena, November

MARKS, W. B. and LOEB, G. E. (1976) Action currents and internodal potentials derived for myelinated mammalian nerve fibres: Implications for extracellular records. *Biophys. J.* **16**, 655–668

PAINTAL, A. S. (1966) The influence of diameter of medullated nerve fibres of cats on the rising and falling phases of the spike and its recovery. *J. Physiol.* (*Lond*) **184**, 791–811

PAINTAL, A. S. (1967) A comparison of the nerve impulses of the mammalian non-medullated nerve fibres with those of the smallest diameter medullated fibres. *Ibid.* **193**, 523–533

PLONSEY, R. (1974) The active fibre in a volume conductor. *IEEE Trans.* **BME-21**, 371–381

ROBINSON, D. A. (1968) The electrical properties of metal microelectrodes. *Proc. IEEE* **56**, 1065–1071

SALCMAN, M. and BAK, M. J. (1973) Design and fabrication and *in vivo* behaviour of chronic recording intracortical microelectrodes. *IEEE Trans.* **BME-20**, 253–260

SANDERS, F. K. and WHITTERIDGE, D. (1946) Conduction velocity and myelin thickness in regenerating nerve fibres. *J. Physiol.* (*Lond*) **105**, 152–174

SCHMIDT, E. M. (1971) An instrument for separation of multiunit neuroelectric signals. *IEEE Trans.* **BME-18**, 155–157

STEIN, R. B. and PEARSON, K. G. (1971) Predicted amplitude and form of extracellularly recorded action potentials from unmyelinated nerve fibres. *J. Theor. Biol.* **32**, 539–558

TASAKI, I. (1964) A new measurement of action currents developed by single nodes of Ranvier. *J. Neurophysiol.* **27**, 1199–1206

THOMAS, C. A. Jun., SPRINGER, P. A., LOEB, G. E., BERWALD-NETTER, Y. and OKUN, L. M. (1972) A miniature microelectrode array to monitor the bioelectric activity of cultured cells. *Exp. Cell Res.* **74**, 61–66

VIZOSO, A. D. and YOUNG, J. Z. (1948) Internode length and fibre diameter in developing and regenerating nerves. *J. Anat. Lond.* **82**, 110–134

WISE, K. D., ANGELL, J. B. and STARR, A. (1970) An integrated circuit approach to extracellular microelectrodes. *IEEE Trans.* **BME-17**, 238–247

Analyse et conception micro-électronique d'ensembles d'électrodes tubulaires destines a l'enregistrement permanent a plusieurs unites separées des fibres nerveuses captées

Sommaire—Cet article examine des propositions pour l'enregistrement de plusieurs potentiels indépendants captés par un ensemble d'électrodes tubulaires. Le captage peut s'effecteur par régénération des fibres coupées ou par le positionnement de filaments disséqués dans des sillons qui sont ensuite recouverts. Les facteurs contribuant aux rapports signal/bruit que l'on peut obtenir avec ce genre d'électrode sont étudiés. La conception, la construction et les résultats d'essais au banc sont exposés pour un ensemble d'électrodes pour lequel on a fait appel à des techniques employant une pellicule micro-électronique mince afin de construire un ensemble d'électrodes tridimensionnel, compact et souple, composé d'un faisceau de tubes en plastique comportant des contacts métalliques plats à mi-longueur du tube.

Analyse und mikroelektronische Konstruktion von Elektrodenanordnungen für Mehrfach-Einzeleinheitsaufzeichnung von gefangenen Nervenfasern

Zusammenfassung—Diese Arbeit behandelt Vorschläge für die Aufzeichnung von Mehrfach-Einzeleinheitspotentialen von Nervenfasern, die in einer Anordnung von Röhrenelektroden gefangen werden. Einfangen kann durch Regeneration von geschnittenen Fasern geschehen oder indem zerlegte Fäden in Rillen gelegt werden, die dann bedeckt werden. Es werden die Faktoren besprochen, die bei diesem Elektrodentyp zum Rauschabstand beitragen. Die Entwurfs-, Konstruktions- und Werkbanktestresultate werden für eine Elektrodenanordnung gegeben, in der Dünnfilm-Mikroelektronikverfahren verwendet werden, um eine dichtgepackte, elastische, dreidimensionale Elektrodenanordnung zu bauen, die aus einem Bündel von Kunststoffröhren mit flachen Metallkontakten in der Röhrenmitte bestehen.